

Distinguishing Graph States by the Properties of Their Marginals

Lina Vandré^{*},¹ Jarn de Jong^{*},² Frederik Hahn,² Adam Burchardt,³ Otfried Gühne,¹ and Anna Pappa^{2,4}

¹Naturwissenschaftlich-Technische Fakultät, Universität Siegen, Walter-Flex-Straße 3, 57068 Siegen, Germany

²Electrical Engineering and Computer Science Department,

Technische Universität Berlin, 10587 Berlin, Germany

³QuSoft, CWI and University of Amsterdam, Science Park 123, 1098 XG Amsterdam, the Netherlands

⁴Fraunhofer Institute for Open Communication Systems - FOKUS, 10589 Berlin, Germany

(Dated: June 17, 2024)

Graph states are a class of multi-partite entangled quantum states that are ubiquitous in many networking applications; the study of equivalence relations between graph states under local operations aims to provide methods to relate graph states in networked settings. The problem of determining local unitary (LU) equivalence of graph states is in NP, and it remains an open question if efficient general methods are possible. We introduce a family of easy-to-compute LU-invariants based on the marginal structure of the graphs that allow to rule out equivalence of graph states. We show that these invariants can uniquely identify all LU-orbits and entanglement classes of every graph state of 8 qubits or less and discuss how reliable the methods are for more qubit graph states. We also discuss examples of entanglement classes with more nodes, where their marginal structure does not allow us to tell them apart. Additionally, we generalise tools to test local clifford (LC) equivalence of graph states that work by condensing graphs into other graphs of smaller size. We show that statements on the equivalence of the smaller graphs (which are easier to compute) can be used to infer statements on the equivalence of the original, larger graphs.

I. INTRODUCTION

Multipartite entanglement plays an important role in many applications of quantum information; it is used for example to generate secret keys between multiple parties in quantum networks [1] and as a resource for measurement based quantum computing [2] and error correction [3] schemes. However, characterising entanglement between more than three parties is not at all straightforward [4, 5]. A fundamental challenge is that the size of the density matrix increases exponentially with the number of parties, making it difficult to simulate large entangled states on classical computers.

Graph states [6] are a subset of multipartite entangled states with useful properties. They have a convenient graphical representation, and, even though they are not as computationally hard to classically simulate as general entangled states, they are used in many of the above-mentioned applications. Graph states can be treated with respect to associated graphs; the association between graphs and graph states (Fig. 1) will be analysed later.

In general, the protocols that use entangled states implement specific operations that can be classified as either local or global. Local operations affect single qubits and are easier to perform. In contrast, global operations target multiple qubits and require them to be in close proximity to be feasible. In scenarios such as key generation, where participants are separated by distance, one is typically limited to local operations. In such remote settings, it is relevant to determine whether a given entangled state can be transformed into a different state

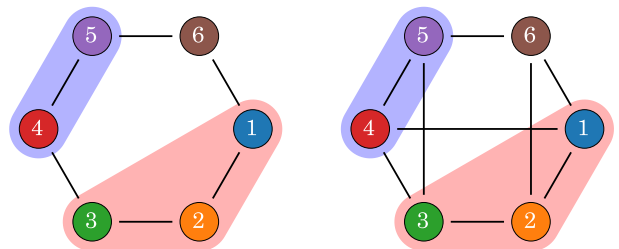


Figure 1. *Graph states* are a certain kind of multipartite entangled states where qubits are represented by nodes of a graph, and the graphs' edges represent entangling gates. We are interested in finding out which graphs correspond to states that share the same entanglement properties, or more precise, if they are equivalent under local unitary operations. In our methods of determining equivalence an integer number d can be assigned to every subset of nodes, which is necessarily the same if the corresponding states have the same entanglement properties. The subsets highlighted in purple have the same number $d_{\{4,5\}}$ for both graphs in the figure, so no conclusion can be drawn yet. However the two graphs have different number $d_{\{1,2,3\}}$ for the subsets highlighted in red. Thus, the two associated graph states can not be equivalent under local unitary operations.

by applying local operations only possibly assisted by classical communication, a setting commonly known as *LOCC*, or *SLOCC* when stochastic transformations are considered that succeed with a non-unit probability. In a first approximation, one can consider merely the set of local unitary (LU) operations, which do not make use of communication between the parties, nor of generalised single-qubit quantum channels. For checking equivalence of two pure multi-qubit states under LU operations a constructive algorithm exists, where LU-equivalence can

^{*}These authors contributed equally to this work.

be decided by solving a finite set of equations [7]. A minimal number of polynomial equations needed to decide LU-equivalence of n -qubit states is discussed in [8].

Perhaps surprisingly, the equivalence of graph states under SLOCC and LU operations coincide [6], so that only LU operations need to be considered in determining the equivalence of two graph states. Moreover, in many cases it is interesting to look at a specific subset of LU operations, known as local Clifford (LC) operations. These are the subset of LU transformations that map the set of multi-qubit Pauli eigenstates to itself and, more importantly, have a clear graphical interpretation [9], providing a powerful tool in the study of equivalence of graph states. By applying LU or LC operations, a given graph state can be transformed into several other graph states. The collection of all the graph states that can be reached from a given starting state is called the LU/LC-orbit of the starting state. Graph states in the same LU/LC-orbit are called *LU/LC-equivalent*. It was once conjectured that LU and LC orbits for graph states coincide [10], but this conjecture has been disproved by finding counterexamples with 27 or more qubits [11, 12]. Still, for states with 8 or fewer qubits, LU and LC orbits do coincide [13]. Determining the orbit of a given graph state is a hard problem, even when restricting to just LC operations: even counting the number of graph states in an LC-orbit is shown to be #P-complete [14] and therefore at least as hard as a NP-complete problem. Still, an efficient polynomial algorithm capable of determining LC-equivalence between two input graphs was discovered by Bouchet [15] and popularised in the physics community in Ref. [16].

Despite the mentioned general methods for demonstrating the LU-equivalence of generic states [7], devising an efficient algorithm to ascertain LU-equivalence remains an unresolved challenge. Earlier works [17, 18] explored the connection between multipartite entanglement of graph states and specific graph-theoretical properties. Following these investigations, studies have been performed [19, 20] on how to distinguish some non-LU-equivalent states based on the entanglement properties of higher order marginals, while a recent paper [21] provided polynomial invariants to negatively answer questions about both LC and LU equivalence in certain cases based on two-body marginal properties.

In this manuscript, we present a systematic approach to characterize LU equivalence of graph states based on properties of their marginals. Our methods contribute to a better visual understanding of entanglement properties in graph states. Furthermore, our methods scale polynomially in the number of nodes and linearly in the number of graphs we wish to compare.

The article is structured as follows. In Sec. II we introduce graphs, graph states, LU and LC-equivalence as well as marginal states. In Sec. III we explain tools that can be used to decide LU-equivalence and discuss in Sec. IV how to detect LU inequivalence even if our methods based on marginals do not work. We continue

introducing graph simplification tools which are invariant under LC transformations in Sec. V. We discuss the computational equivalence of our tools in Sec. VI and conclude our work with a summary in Sec. VII.

II. PRELIMINARIES

A. Graphs and Metagraphs

Definition 1. A graph $G = (V, E)$ is a set of vertices V and edges $E \subseteq V \times V$ connecting two vertices.

In this paper we only consider simple connected graphs. Graphs are connected if for any two nodes $i, j \in V$ we can find a path, i.e., a sequence of adjacent edges, that connects them. Graphs are simple if they contain neither self-loops of nodes nor multiple edges between two different nodes. Finally, we note that our methods easily generalise to disconnected graphs.

Two examples of graphs are given in Fig. 3. Graphs can be represented by their adjacency matrices. For a graph with $n = |V|$ nodes, the symmetric $n \times n$ matrix $\Gamma(i, j) = \Gamma(j, i)$ encodes the edges as

$$\Gamma(i, j) = \begin{cases} 1 & \text{if } (i, j) \in E, \\ 0 & \text{otherwise.} \end{cases} \quad (1)$$

The i -th column η_i of Γ indicates node i 's neighbours, with $\eta_i(j) = 1$ if node j is a neighbour, and 0 otherwise. The *neighbourhood* \mathcal{N}_i of a node i is the collection of all other nodes of the graph that share an edge with it:

$$\mathcal{N}_i := \{j \in V \mid (i, j) \in E\}.$$

In the same way, we define the neighbourhood of a set $M \subsetneq V$ as the set of vertices adjacent to at least one vertex in M :

$$\mathcal{N}_M := \{v \in V \setminus M \mid \exists m \in M : (v, m) \in E\}. \quad (2)$$

To ease notation, by $\mathcal{P}(M)$ we denote the power-set of M , i.e. the set $\mathcal{P}(M) = \{N : N \subseteq M\}$ of all subsets of M .

In some cases, we are interested in the structure of a set $M \subset V$ of vertices and its neighbourhood, but not in the entire graph G . For that purpose, we define a metagraph G_M , which depends on a given graph $G = (V, E)$ and a subset of its nodes, $M \subset V$. Such a metagraph consists of two types of nodes. Type-1 nodes are simply the nodes in M . For every non-empty subset $M' \subseteq M$, there exists a type-2 node labelled by that subset between square brackets, i.e., $[M']$. The rules for connecting the nodes of the metagraph are as follows: Type-1 nodes are connected to each other if and only if they are connected in the original graph G . A type-2 node with label $[M']$ is connected to all the type-1 nodes in M that appear in their label $[M']$ if and only if the following condition is met: There exists at least one node v in the original

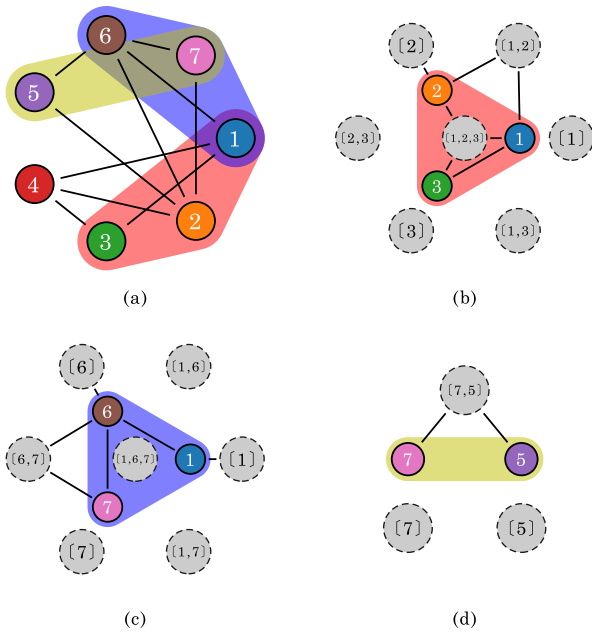


Figure 2. (a) : A graph $G = (V, E)$ with 3 different highlighted sets M , of size 2 and 3. (b), (c), (d) : The highlighted sets M give rise to different metagraphs.

graph G , but outside of M such that the intersection of its neighborhood with M equals M' . If there is no v with this property, the type-2 node $[M']$ remains isolated. Note that there are never edges between two type-2 nodes in a metagraph. Finally, we are also ignorant how many nodes in $V \setminus M$ of the original graph are adjacent to nodes in M . We formalize this definition as follows:

Definition 2 (Metagraph). *For a graph $G = (V, E)$ and a set $M \subsetneq V$ the metagraph of M is defined as the graph $G_M = (M \cup \mathcal{P}(M) \setminus \emptyset, E_M)$, where each node v of G_M is of one of two types: either $v \in M$ or $v \in \mathcal{P}(M) \setminus \emptyset$. The edge set E_M contains all edges of the induced subgraph on M . Furthermore, if in the initial graph G there exists a node $v' \in V \setminus M$ such that $\mathcal{N}_{v'} \cap M = w$, the node $w \in \mathcal{P}(M) \setminus \emptyset$ is connected to all nodes $v \in w$. Otherwise, the node $w \in \mathcal{P}(M) \setminus \emptyset$ remains isolated.*

To see this in an explicit example, we consider the upper right (red) metagraph shown in Fig. 2. The metagraph $G_{\{1,2,3\}}$ has type-1 nodes $M = \{1, 2, 3\}$, as well as type-2 nodes $\mathcal{P}(M) \setminus \emptyset = \{\{1\}, \{1, 2\}, \{1, 2, 3\}, \dots\}$. Between nodes in M , the metagraph has the same edges as G . Edges between nodes in M and $\{\{2\}, \{1, 2\}, \{1, 2, 3\}\}$ can be explained as follows: There is an edge between node $2 \in M$ and node $\{2\} \in \mathcal{P}(M)$, since for node $5 \in V$ of the original graph, we have $\mathcal{N}_5 \cap M = \{2\}$. We further find edges between nodes $1, 2 \in M$ and node $\{1, 2\} \in \mathcal{P}(M)$, since for node $6 \in V$ of the original graph, we have $\mathcal{N}_6 \cap M = \{1, 2\}$. Since $\mathcal{N}_4 \cap M = \{1, 2, 3\}$, we also have edges between nodes $1, 2, 3 \in M$ and node $\{1, 2, 3\} \in \mathcal{P}(M)$.

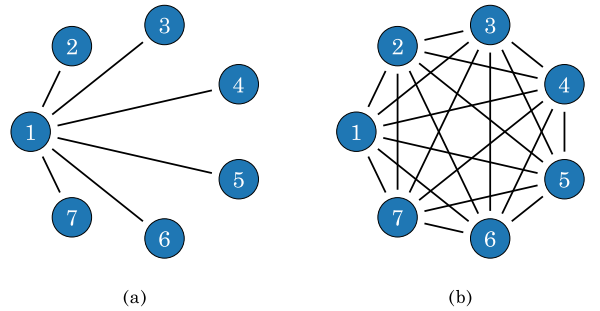


Figure 3. (a) : The *star* graph, whose corresponding graph state is equivalent to the $|\text{GHZ}\rangle$ state. (b) : Local operations on the qubits of the GHZ state result in a different (albeit locally equivalent) graph state, which is represented by the complete graph.

B. Graph States

Graph states are quantum states composed of multiple qubits from a graph $G = (V, E)$, where vertices and edges represent qubits and entangling gates, respectively.

Definition 3. *The graph state corresponding to a graph $G = (V, E)$ is defined as*

$$|G\rangle := \prod_{e \in E} CZ_e |+\rangle^{\otimes |V|}, \quad (3)$$

where CZ_e is a CZ gate, acting on qubits in the edge e .

There is an equivalent definition using stabiliser operators. For each node $i \in V$ we can define a generator,

$$g_i := X_i \bigotimes_{j \in \mathcal{N}_i} Z_j, \quad (4)$$

where X_i , Y_i , and Z_i are the Pauli matrices acting on the i -th qubit and \mathcal{N}_i is the neighbourhood of i . The products of the generators g_i form the *stabiliser* $\mathcal{S}(G)$ – a commutative group with 2^n elements. The graph state $|G\rangle$ is then defined as the unique joint n -qubit $+1$ eigenstate of all generators g_i or simply by

$$|G\rangle\langle G| = \frac{1}{2^n} \sum_{s \in \mathcal{S}(G)} s. \quad (5)$$

A prominent example of a graph state is the Greenberger-Horne-Zeilinger (GHZ) state [22], used in quantum communication protocols to establish secret keys [23, 24], share quantum secrets [25] and communicate anonymously [26, 27]. A n -qubit GHZ state can be represented by a fully connected graph or a star graph of n nodes, as shown in Fig. 3. Another noteworthy example of graph states are cluster states; these are represented by grid-like graphs and play an important role in measurement based quantum computing [28, 29].

C. Equivalence under Local Unitary Operations

Graph states naturally arise in network scenarios, where each node in the network represents a single qubit. Since the nodes are usually spatially distant from each other, studying the effect of *local* operations on graph states is of practical interest.

1. LU-Equivalence

Local operations can transform one graph state into another, which leads to the question whether two graph states are equal up to local operations. More specifically, two graph states $|G_1\rangle$ and $|G_2\rangle$ are *local unitary* or LU-equivalent if and only if $|G_1\rangle = U|G_2\rangle$ and the n -qubit unitary operator $U \in \mathcal{U}(2^n)$ allows a decomposition into a tensor product of single-qubit operations

$$U = \bigotimes_{i=1}^n U_i \quad | U_i \in U(2). \quad (6)$$

For example, the graph states corresponding to the star graph and the fully connected graph of n nodes and the GHZ state in its common form are local unitary equivalent. This can be seen as follows. The n -qubit GHZ state in its standard form is given by

$$|\text{GHZ}_n\rangle = \frac{1}{\sqrt{2}} (|0_1 0_2 \dots 0_n\rangle + |1_1 1_2 \dots 1_n\rangle). \quad (7)$$

For the n -node star graph with the first node as central node (as shown in Fig. 3), one finds

$$|G_{\text{star},n}\rangle = \frac{1}{\sqrt{2}} (|0_1 +_2 \dots +_n\rangle + |1_1 -_2 \dots -_n\rangle). \quad (8)$$

Applying local, unitary Hadamard gates on all qubits except the first, we get $|\text{GHZ}_n\rangle$.

From the aforementioned network perspective, there is an implied labelling of the nodes of the graph by their location. From a less operational but more theoretical perspective, we can also be interested in *unlabelled* graphs. Comparing unlabelled graph states under local operations amounts to studying so-called *entanglement classes*. Two graphs belong to the same entanglement class if there exists an arbitrary permutation of the nodes of the first graph that results in a graph that is in the (LU or LC)-orbit of the second graph.

2. LC-Equivalence and Local Complementation

From the local unitaries we can turn our attention to one of their subsets. The *Clifford group* is the normaliser of the n -qubit Pauli group \mathcal{P}_n in the unitary group $\mathcal{U}(2^n)$:

$$\mathcal{C}_n = \{C \in \mathcal{U}(2^n) | C\mathcal{P}_n C^\dagger = \mathcal{P}_n\}. \quad (9)$$

In practice, this means that Clifford unitaries map strings of Pauli matrices to strings of Pauli matrices.

The Clifford matrices that decompose into single-qubit tensor products form the *local Clifford group* \mathcal{C}_n^l . Two graph states $|G_1\rangle$ and $|G_2\rangle$ are *local Clifford* or LC-equivalent if and only if $|G_1\rangle = C|G_2\rangle$ for some $C \in \mathcal{C}_n^l$.

Remarkably, there is a simple relationship between local Clifford operations on graph states and so-called *local complementations* on their associated graphs [30]. Local complementation of a graph G at node i results in the graph $G' = \text{LC}_i(G)$, where the neighbourhood of i is inverted.

Definition 4. Each vertex $i \in V$ of a graph $G = (V, E)$, defines a locally complemented graph $\text{LC}_i(G)$ with adjacency matrix $\Gamma_{\text{LC}_i(G)} := \Gamma_G + \Gamma_{\mathcal{N}_i} \pmod{2}$, where

$$\Gamma_{\mathcal{N}_i}(j, k) = \begin{cases} 1 & \text{if } j, k \in \mathcal{N}_i, j \neq k \\ 0 & \text{otherwise.} \end{cases} \quad (10)$$

is the adjacency matrix of the complete graph on the neighbourhood \mathcal{N}_i of i and empty on all other vertices.

In other words, local complementation ‘flips’ the adjacency relations between the neighbours of i : if two nodes in \mathcal{N}_i are connected by an edge in G , they are not connected in $\text{LC}_i(G)$, and vice versa. Each LC_i operation only affects the edges in the neighbourhood of i ; all other edges remain unchanged.

There is a one-to-one correspondence between the local complementation orbit of a given graph and the orbit under local Clifford operations of the corresponding graph state [30]. The explicit local Clifford operation $\text{LC}_i \in \mathcal{C}_n^l$ corresponding to a local complementation is given by

$$\text{LC}_i = \sqrt{-iX_i} \bigotimes_{j \in \mathcal{N}_i} \sqrt{iZ_j}. \quad (11)$$

An example of local complementation is shown in Fig. 3. If we perform local complementation on the central node of the star graph, all other nodes get pairwise connected, which results in the fully connected graph. Local complementation in for example node 2 of the star graph does not change the graph. Local complementation on any node i of the fully connected graph leads to a star graph with node i as the center. We previously showed that the star graph state is LU equivalent to the GHZ state in its common form. Applying local complementation shows that also the fully connected graph state is LC- (and therefore particularly LU-) equivalent to the GHZ state.

Note that the effect of an arbitrary local Clifford on a graph state does not have to result in a graph state again. In general, the effect of local Cliffords on graph states will result in different stabiliser states.

Fortunately, every stabiliser state is itself LC-equivalent to some graph state, and such graph states can be found efficiently [30]. Since this relation is not unique, we say that a stabiliser state is LC-equivalent to a graph state orbit.

Combining this insight with the efficient algorithm [15] for determining whether two graphs are in each other's local complementation orbit results in an efficient method for determining whether two stabiliser states are LC-equivalent [31].

D. Marginal States

In the following section we discuss how structural properties of graphs are related to properties of reduced density matrices (i.e. marginals) of graph states,

Definition 5. *The marginal state ρ_M on a proper subset of vertices $M \subsetneq V$ is defined as*

$$\rho_M(G) := \text{Tr}_{V \setminus M}(|G\rangle\langle G|) = \frac{1}{2^n} \sum_{S \in \mathcal{S}(G)} \text{Tr}_{V \setminus M}(S), \quad (12)$$

where $\text{Tr}_{V \setminus M}$ is the trace over all systems in $V \setminus M$.

Since Pauli matrices are traceless, for sufficiently small M we have $\text{Tr}_{V \setminus M}(S) = 0$ in many cases. There are a few special cases, where the partial trace is not zero. For the trivial stabiliser $\mathbb{1}_V \in \mathcal{S}$ we have $\text{Tr}_{V \setminus M}(\mathbb{1}_V) = 2^{|V \setminus M|} \mathbb{1}_M$, where the index of $\mathbb{1}$ indicates the size of the identity matrix. Depending on the choice of M , there may be stabilisers whose non-trivial support is contained in M , i.e. all indices of Pauli matrices are contained in M . In this case the partial trace is also different from zero.

The *reduced stabiliser* is the subgroup $\mathcal{S}_M \subseteq \mathcal{S}$ defined

$$\mathcal{S}_M := \{S \in \mathcal{S}(G) : \text{Tr}_{V \setminus M}(S) \neq 0\} \quad (13)$$

$$= \{S \in \mathcal{S}(G) : \text{supp}(S) \subset M\}, \quad (14)$$

where $\text{supp}(S)$, the *support* of a Pauli operator S , is the collection of tensor-subspaces on which it acts non-trivially. Directly from the definition, it follows that \mathcal{S}_M forms a group. Every element of \mathcal{S}_M squares to the identity and commutes with any other element, and therefore the order of the group \mathcal{S}_M is a power of two. Consequently, we can define the following integer number

$$d_M := \log_2(|\mathcal{S}_M|), \quad (15)$$

as the rank of the group \mathcal{S}_M , i.e., the minimum number of elements in a generating set of \mathcal{S}_M .

\mathcal{S}_M is an abelian subgroup of \mathcal{S} with at most $2^{|M|}$ elements. Therefore, and if M is a proper subset of V , we have the equation

$$0 \leq d_M < |M|, \quad (16)$$

where the last inequality is strict because we only consider connected graphs. This also allows for a straightforward check of connectedness: if and only if a graph is disconnected over the partition $M : M'$, we have $d_M = |M|$.

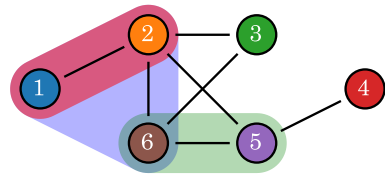


Figure 4. Example for marginal states on a six node graph. The state $\rho_{\{1,2\}}$ is stabilised by $\mathcal{S}_{\{1,2\}} = \{\mathbb{1}, g_1\}$. The state $\rho_{\{1,2,6\}}$ is stabilised by $\mathcal{S}_{\{1,2,6\}} = \{\mathbb{1}, g_1, g_2g_6, g_1g_2g_6\}$. The state $\rho_{\{5,6\}}$ is stabilised by $\mathcal{S}_{\{5,6\}} = \{\mathbb{1}\}$. The stabilisers are given by $g_1 = X_1Z_2$, $g_2g_6 = -Z_1Y_2Y_6$, and $g_1g_2g_6 = Y_1X_2Y_6$

Notice that group \mathcal{S}_M defines respective marginal state. Indeed, by Eq. (12), we have

$$\rho_M(G) = \frac{1}{2^{|M|}} \sum_{S \in \mathcal{S}_M} \text{Tr}_{V \setminus M}(S). \quad (17)$$

An example for marginal states is given in Fig. 4. Computing one- and two- body marginals of graph states was discussed in details in Ref. [32].

III. TOOLS FOR CHARACTERIZING LU EQUIVALENCE

We are interested in which graph states can or can not be transformed into other graph states using local unitary operations. LU equivalent graph states have in general different reduced states, but certain properties stay invariant under local unitary operations. For example the number of stabiliser elements in $|\mathcal{S}_M|$ or the rank of the reduced state are invariant under LU transformations. In the following we utilize these invariant properties to distinguish between graph states that are not LU-equivalent.

Recall the following relation between the rank of reduced density matrix ρ_M and the size of stabiliser subgroup \mathcal{S}_M :

$$\text{rank}(\rho_M) = 2^{|M| - d_M}. \quad (18)$$

The rank of a reduced density matrix is invariant under LU operations, thereby ensuring that the dimension d_M also is invariant under such operations.

Sometimes it will be useful to calculate the marginal dimension d_M from the adjacency matrix Γ . Without loss of generality, we assume that the nodes in M are the first $|M|$ indices of Γ ; the rest is indexed by $M^\perp = V \setminus M$. We can then write the adjacency matrix in block form:

$$\Gamma = \begin{bmatrix} \Gamma_{M,M} & \Gamma_{M,M^\perp} \\ \Gamma_{M^\perp,M} & \Gamma_{M^\perp,M^\perp} \end{bmatrix}, \quad (19)$$

where $\Gamma_{A,B}$ denotes the submatrix of the adjacency matrix Γ with rows and columns indexed by subsets A and

B respectively. We can calculate the dimension of d_M as follows [6]:

$$d_M = \text{Null}(\Gamma_{M^\perp, M}) = |M| - \text{rank}(\Gamma_{M, M^\perp}), \quad (20)$$

where $\text{Null}(A)$ denotes the nullity of a matrix A , i.e. the dimension of its kernel, calculated over the binary field.

In order to determine the dimension d_M , we can also use the adjacency matrix Γ^{G_M} of the corresponding meta-graph G_M . Indeed, we have

$$\text{rank}(\Gamma_{M, M^\perp}) = \text{rank} \Gamma_{M, \mathcal{P}(M)}^{G_M} \quad (21)$$

where $\Gamma_{M, \mathcal{P}(M)}^{G_M}$ denotes the submatrix of the adjacency matrix Γ^{G_M} with rows and columns indexed by vertices in M and columns indexed by subsets of M . This can be easily seen, as the matrix $\Gamma_{M, \mathcal{P}(M)}^{G_M}$ is obtained from Γ_{M, M^\perp} by deleting repetitive columns, see Def. 2.

We conclude this section with outlining the following relation between the marginal dimension d_M and the entanglement entropy $E_M(|G\rangle)$ with respect to the bipartition $M|M^\perp$:

$$E_M(|G\rangle) := -\text{Tr}(\rho_M \log_2 \rho_M) = |M| - d_M. \quad (22)$$

From the fact that $E_M(|G\rangle) = E_{M^\perp}(|G\rangle)$ we get the equality

$$d_{M^\perp} = d_M + |M^\perp| - |M|. \quad (23)$$

A. Characterizing LU-orbits by Their Rank Invariants

In this section, we discuss how we can use the mentioned invariant measures to distinguish between different LU-orbits of graph states. For a given graph $G = (V, E)$, we denote by

$$L_i^{k, G} = \{M \subseteq V : |M| = k, d_M = i\} \quad (24)$$

the collection of all subsets $M \subseteq V$ of vertices of size $|M| = k$ such that the corresponding marginal ρ_M is of dimension $d_M = i$. Furthermore, for given value k , we define

$$l_k^G = \left(|L_0^{k, G}|, \dots, |L_k^{k, G}| \right), \quad (25)$$

which is a vector of dimensions of sets $L_i^{k, G}$ for all values $0 \leq i \leq k$.

Moreover, for any graph $G = (V, E)$ and number k , $0 \leq k \leq n$, we define k -dimensional tensor

$$T_k^G = (t_{i_1 \dots i_k})_{i_1, \dots, i_k \in V} \quad (26)$$

with entries determined by the dimensions of the corresponding marginals, i.e

$$t_{i_1 \dots i_k} := d_{\{i_1, \dots, i_k\}}. \quad (27)$$

Notice that elements i_1, \dots, i_k are not necessarily pairwise different, hence the set $M = \{i_1, \dots, i_k\}$ might be of any size $1 \leq |M| \leq k$. Therefore tensor T_k^G contains the information about the size of dimensions of all marginal states ρ_M corresponding to the subsets $M \subseteq V$ of size $|M| \leq k$. Notice that for any k , the tensor T_{k-1}^G is embedded into the (generalized) diagonals of T_k^G , and that T_k^G is super-symmetric, i.e $t_{i_1 \dots i_k} = t_{\sigma(i_1) \dots \sigma(i_k)}$ for arbitrary permutation σ .

It is worth mentioning some alternative concepts akin to tensors T_k^G , such as the sector length [33] and cut-rank [34, 35] of a graph, which merit acknowledgment.

For distinguishing LU-orbits, we have the following lemma:

Lemma 6. *Consider two labelled graphs $G = (V, E)$ and $G' = (V, E')$ defined on the same node set V . If the corresponding graph states $|G\rangle$ and $|G'\rangle$ are LU-equivalent, we have*

$$L_i^{k, G} = L_i^{k, G'}, \quad (28)$$

for all marginal sizes $k \in \{0, \dots, n\}$ and marginal dimensions $i \in \{0, \dots, k-1\}$. Similarly, we have

$$T_k^G = T_k^{G'}. \quad (29)$$

Because of Eq. (23), any T_k^G for $k > \lfloor \frac{n}{2} \rfloor$ can be directly computed from T_{n-k}^G .

Note that this gives only a *necessary* condition for LU-equivalence, but not a sufficient one. When the graphs have a marginal state with different dimensions, we can conclude they do not belong to the same LU-orbit. The converse is not true: two graphs with exactly the same marginal ranks are not necessarily LU-equivalent. The smallest counter-example are two graphs of 9 nodes, we refer to Sec. IV for more details.

As an example of the usage of Lem. 6, the left and middle graphs in Fig. 5 belong to the same LU-orbit, and thus have the same marginal ranks. The right graph is not LU-equivalent: the two highlighted marginals have $d_{(1,3)} = d_{(2,3)} = 0$, whereas the other two graphs have $d_{(1,3)} = d_{(2,3)} = 1$.

It can happen that two different orbits give the same two-body marginal ranks, but that higher-order marginals are different. In telling apart different LU-orbits, it is therefore sometimes necessary to increase the marginal size. For instance, the dimensions of all the 2-body marginals from both graphs in Fig. 1 are the same. However, some of the 3-body marginals have different dimensions; the left graph has $d_M = 1$ on the highlighted 3-body set, whereas the right graph (corresponding to the absolutely maximally entangled state of six qubits) has $d_M = 0$ for the same set.

Lem. 6 is considerably easier to check for labeled graphs; for unlabelled graphs we additionally need to verify that we are comparing sets of associated vertices; there are generally a super-exponential number of these. However, there are ways to relax Lem. 6 so that it becomes more suitable for unlabelled graphs. We already

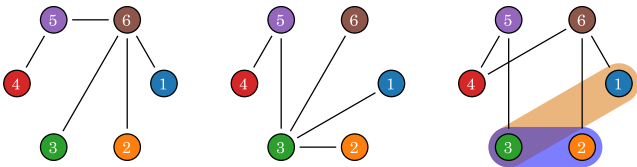


Figure 5. The graph on the left and in the middle have the same two-body marginal dimensions $d_{|M|=2}$; they also belong to the same LU-orbit (more specifically, they are related by a local complementation on node 6 (brown), followed by a local complementation on node 3 (green)). The graph on the right has certain marginals with a different dimension from the other two graphs: the highlighted two-body marginals $M_1 = \{1, 3\}$ and $M_2 = \{2, 3\}$ have $d_M = 0$ for the right graph, instead of $d_M = 1$ for the other two graphs.

have that l_k is invariant under permutations of the nodes of the underlying graph, and as such constant when evaluated over elements in an entanglement class. However, T_k will generally not be invariant under these permutations. We first derive a permutation-invariant measure from the tensor T_k :

Definition 7. Consider a marginal tensor T_k^G as defined in Eq. (26). Let $\{\lambda_1, \dots, \lambda_k\}$ be the (real) eigenvalues of the Hermitian matrix we get after summing over $k - 2$ arbitrary axes of the tensor. Then we define t_k^G as the product of nonzero eigenvalues λ_i :

$$t_k^G = \prod_{\lambda_i \neq 0} \lambda_i. \quad (30)$$

Note that the eigenvalues are invariant under permutation of the marginal tensor T_k^G .

We are now ready to state a corollary of Lem. 6 containing two LU-invariant measures that are equal up to permutations of the nodes, i.e. constant over elements of an entanglement class.

Corollary 8. Consider two unlabelled graphs $G = (V, E)$ and $G' = (V, E')$ defined on the same node set V . If the corresponding graph states $|G\rangle$ and $|G'\rangle$ are LU-equivalent, we have

$$l_k^G = l_k^{G'}, \quad (31)$$

$$t_k^G = t_k^{G'}. \quad (32)$$

Cor. 8 can be used to test if two unlabelled graph states belong to the same entanglement class. Fig. 6 contains two unlabelled graphs that do not belong to the same entanglement class: they have a different valued l_2 , and thus cannot belong to the same class.

We now investigate to which extent the knowledge of the dimensions of the complete set of k -body marginals of a labelled or unlabelled LU-orbit allows to characterize that orbit (or class). For a given labelled graph state, does its marginal tensor T_k uniquely correspond to its own LU-orbit, so that any graph state from another LU-orbit has a different T_k ? Similarly, for an unlabelled

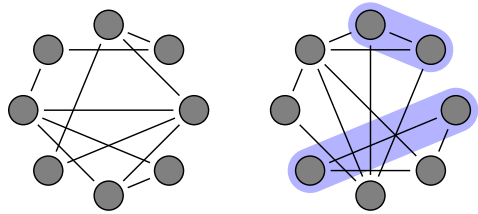


Figure 6. The unlabelled graphs, G (left) and G' (right) belong to different entanglement classes. The left graph has $l_2^G = [21, 0]$, whereas the right graph has $l_2^{G'} = [19, 2]$; the two marginals with $d = 1$ have been highlighted. Note that purely the inequality $l_2^G \neq l_2^{G'}$ is enough to conclude that G and G' do not belong to the same entanglement class.

graph state, does its (permutation-invariant) measure l_G or t_G correspond uniquely to its own entanglement class?

To test how well the presented invariants perform in distinguishing different LU-orbits (for T_k) or classes (for l_k and t_k), and comparing graphs for equivalence, we introduce two figures of merit; these can be computed for the aforementioned invariants, for any graph size n and marginal size k :

- The ratio of different invariants, divided by the total number of LU-orbits (for T_k) or entanglement classes (for l_k and t_k). We denote this $r(T_k)$, $r(l_k)$ or $r(t_k)$.
- The probability that, given two random graph states $|G\rangle$ and $|G'\rangle$, their invariants are evaluated at the same value, even though they do not belong to the same LU-orbit (for T_k) or entanglement class (for l_k and t_k). We denote this $p(T_k)$, $p(l_k)$ or $p(t_k)$.

We compute the marginal tensors of a representative of every LU-orbit for $k \in \{2, \dots, \lfloor \frac{n}{2} \rfloor\}$, up to 9 qubits. Entanglement class representatives are sourced from the supplementary material of [36]; the representatives of the associated orbits are computed from these by exhaustive search through all permutations.

Subsequently we compute the figures of merit $r(T_k)$ and $p(T_k)$. If $r(T_k) = 1$ it means that every LU-orbit has a unique tensor T_k to identify it, whereas it is one divided by the number of orbits when all different LU-orbit have the same marginal tensor T_k . Similarly, if $p(T_k) = 0$ it means that two random non-LU-equivalent graph states always will have a different T_k , while when $p(T_k)$ is close to one, it is very likely that the two graph states will have the same T_k . See Tbl. I for the results.

Similarly to the LU-orbits, we compute l_k and t_k for a representative of every entanglement class, and compute the figures of merit $r(l_k)$, $r(t_k)$, $p(l_k)$ and $p(t_k)$. These results are given in Tbl. II for l_k and in Tbl. III for t_k .

We see that for labeled graphs, our methods work can perfectly distinguish all LU-orbits up to eight qubits, provided that marginals of a large enough size are used. At the same time, the number of different invariants versus

n	$r(T_2)$	$r(T_3)$	$r(T_4)$	$p(T_2)$	$p(T_3)$	$p(T_4)$
3	1	-	-	0	-	-
4	1	-	-	0	-	-
5	1	-	-	0	-	-
6	0.52	1	-	0.05	0	-
7	0.13	1	-	0.12	0	-
8	0.02	0.88	1	0.22	0.0001	0
9	0.001	0.48	0.999	0.37	0.0004	3e-10

Table I. For labelled graphs of size $n \geq 3$ and marginal size $k \leq \lfloor \frac{n}{2} \rfloor$, we compute $r(T_k)$ and $p(T_k)$. If $r(T_k) = 1$, each LU -orbit uniquely corresponds to a specific T_k , serving as its identifier. Similarly, if $p(T_k) = 0$, any two non- LU -equivalent graph states will have a different T_k .

n	$r(l_2)$	$r(l_3)$	$r(l_4)$	\mathbf{R}	$p(l_2)$	$p(l_3)$	$p(l_4)$	\mathbf{P}
3	1	-	-	1	0	-	-	0
4	1	-	-	1	0	-	-	0
5	1	-	-	1	0	-	-	0
6	0.73	0.82	-	1	0.01	0.01	-	0
7	0.42	0.85	-	0.92	0.17	0.03	-	0.03
8	0.15	0.54	0.56	0.94	0.30	0.05	0.03	0.01
9	0.04	0.34	0.70	0.83	0.44	0.05	0.01	0.01

Table II. The table details the computation of $r(l_k)$ and $p(l_k)$ for unlabelled graphs with sizes $n \geq 3$ and marginal sizes $k \leq \lfloor \frac{n}{2} \rfloor$, applying prior definitions for r and p . It identifies entanglement classes using l_k as unique markers or distinctions between classes. The \mathbf{R} and \mathbf{P} columns show the aggregated r ratios and p probabilities for class identification.

the number of different orbits (i. e. $r(T_k)$) diverge fast: e.g. $r(T_2)$ equals 1 for up to five qubits, but becomes 0.002 for eight qubits.

From nine qubits, the methods fail to label all classes differently. This is a direct consequence of the fact that for nine qubits there are (up to permutations) two separate orbits that have the exact same marginal structure; these classes are discussed in more detail in Sec. IV, where it is proven that they are in fact LU -inequivalent in addition to being LC -inequivalent.

n	$r(t_2)$	$r(t_3)$	$r(t_4)$	\mathbf{R}	$p(t_2)$	$p(t_3)$	$p(t_4)$	\mathbf{P}
3	1	-	-	1	0	-	-	0
4	1	-	-	1	0	-	-	0
5	1	-	-	1	0	-	-	0
6	0.73	1	-	1	0.01	0	-	0
7	0.46	1	-	1	0.16	0	-	0
8	0.19	0.89	1	1	0.30	0.0001	0	0
9	0.06	0.73	0.998	0.998	0.44	0.01	1e-06	1e-06

Table III. The table calculates $r(t_k)$ and $p(t_k)$ for unlabelled graphs of size $n \geq 3$ with marginal size $k \leq \lfloor \frac{n}{2} \rfloor$, leveraging earlier definitions for r and p . It distinguishes entanglement classes using eigenvalues t_k as unique identifiers or indicators of different classes. Columns \mathbf{R} and \mathbf{P} present combined ratios r and probabilities p for class identification.

Turning to the second figure of merit (i.e. the right side of Tbl. I), we also see that up to 8 qubits there is always a marginal size such that the probability of a false positive becomes zero. This is a direct consequence of the left side of the table, more specifically that $r(T_k)$ can equal 1 for all these cases. Here, a false positive is the case that two (randomly chosen) graphs are identified as belonging to the same orbit, without that being the case. The results differ, however, when the ratios and probabilities are not zero. For instance, for 7 qubits $r(T_2)$ is only 0.13, but still there is only a twelve percent probability that two random but non- LU -equivalent graphs have the same T_2 . This disparity is explained by the fact that the orbits differ in size: the smallest orbit is the GHZ orbit with 8 graphs, of which two elements are shown in Fig. 3. The largest orbit, of which there are 105 permutational copies, contains 1096 graphs. This effect seems to get stronger with larger graphs. For 9 qubits, the number of different T_2 's is only 0.1% of the total number of orbits. Still, the probability of a false positive is less than half. Similarly, $r(T_3)$ is roughly half, but the chance of a false positive is negligible.

For unlabelled graphs (i.e. entanglement classes) we see similar behaviour. First considering l_k , we see similar scaling as for labelled graphs: the number of different invariants versus the number of different classes diverge fast, and the probabilities for a false positive increase slower. Only classes up to 6 qubits can be perfectly distinguished, which is less than for the orbits. Nevertheless, the expected behaviour is returned when considering t_k instead: here, again all classes up to and including 8 qubits can be perfectly distinguished.

A surprising property is that for comparing lists, we note that the reliability of our results increase, if we consider lists of several marginal set sizes k together at the same time. For example for 8 node graphs, the ratio r_k is below 60% for each k equal to 2, 3, and 4. However, combining all three lists gives a ratio of 94%. One reason is that the information given in a list l_k can only partly be estimated by a list of higher $k' > k$. This behaviour is not apparent in T_k (and by extension t_k), because T_{k-1} is 'embedded' into the (higher-dimensional) diagonal of T_k .

B. Characterizing LU -orbits by Their Graph Structures

A visual tool to distinguish graph states are meta-graphs. We can directly derive the set \mathcal{S}_M of a marginal set M from its meta-graph. We can further group meta-graphs into meta-orbits, which is a method to distinguish graphs. In this section we discuss how to derive \mathcal{S}_M for general sets M . We further present the meta-graph orbits of sets of size two and three and discuss how our observations are connected to the results of the previous section.

1. Computing the Marginal Dimension Graphically

A metagraph of a set $M = \{1, 2\}$ has three type-2 nodes: $\mathcal{P}(\{1, 2\}) \setminus \emptyset = \{\{1\}, \{2\}, \{1, 2\}\}$. The marginal ρ_M can at most get stabilised by $\mathbb{1}, g_1, g_2$, and g_1g_2 , since all other stabiliser elements g_j for $j \notin M$ vanish in the partial trace. We determine which of the stabiliser elements do not vanish from the non-empty neighboursets. The stabiliser element g_1 does not vanish if the type-2 nodes $\{1\}$ and $\{1, 2\}$ are not connected to type-1 nodes in M . This is the only case where g_1 has support on M and no support outside, that is $g_1 = X_1Z_2$. An equivalent argumentation can be done for g_2 . The stabiliser element g_1g_2 does not vanish if the type-2 nodes $\{1\}$ and $\{2\}$ are not connected to type-1 nodes in M . Depending on whether type-1 nodes 1 and 2 are connected or not, g_1g_2 is given by Y_1Y_2 or X_1X_2 , respectively, which has support on M . The case of two node sets was already discussed in Ref. [32].

For example the lower right (yellow) metagraph shown in Fig. 2(d) has $\{5, 7\}$ as only type-1 node connected to $M = \{5, 7\}$. This indicates that the marginal $\rho_{\{5,7\}}$ is stabilised by $\mathcal{S}_{\{5,7\}} = \{\mathbb{1}, g_5g_7\}$. It follows that $d_{\{5,7\}} = 1$.

This concept can get generalised to an arbitrary set M . The marginal state ρ_M can in principle get stabilised by stabiliser elements $\{g_L \mid L \subseteq M\}$, where $g_L := \prod_{i \in L} g_i$. A stabiliser element g_L has support on M if and only if all type-2 nodes which are connected to M are either connected to an even number of type-1 nodes in L or are not connected to nodes in L . That is g_L is in \mathcal{S}_M if and only if all type-2 nodes $w \in \mathcal{P}(M)_{k \geq 0}$ for which $|w \cap L|$ is an odd number are not connected to type-1 nodes in M . Note that a similar definition was given in Ref. [37].

For example the metagraph (b) in Fig. 7 has two type-2 nodes $\{\{1, 2\}, \{2, 3\}\}$ connected to the set $M = \{1, 2, 3\}$. This graph gets stabilised by $g_{L=\{1,2,3\}} = g_1g_2g_3$, since $|\{1, 2\} \cap \{1, 2, 3\}| = |\{2, 3\} \cap \{1, 2, 3\}| = 2$. All other subsets $L \subseteq M$, which are not the empty set have an odd number of elements in the intersection with $\{1, 2\}$ or $\{2, 3\}$ and therefore there are no other stabilisers than $\mathbb{1}$.

An alternative definition of the stabiliser set (already defined in Eqs. (13) and (14)) is given by

$$\mathcal{S}_M := \left\{ g_{L \subseteq M} \mid \begin{array}{l} \forall w \in \mathcal{P}(M)_{k \geq 0} \text{ connected to } M : \\ |N \cap w| \text{ is even} \end{array} \right\}. \quad (33)$$

Therefore we can reproduce the results discussed in the previous chapter from metagraphs.

2. Marginal Orbits

A deeper look into graph structures can be taken by considering marginal orbits.

Definition 9 (Marginal orbit). *Two metagraphs G_M and G'_M belong to the same marginal orbit, if there are*

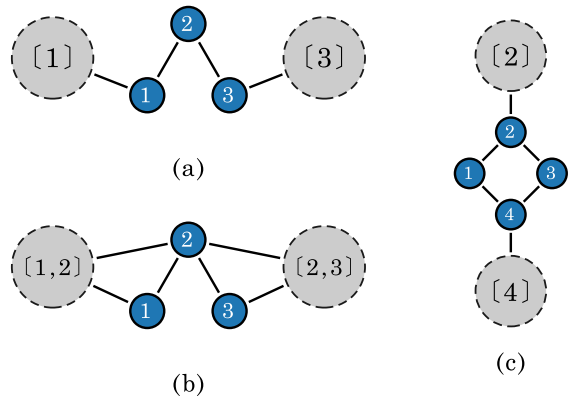


Figure 7. Example of new structures detected by marginals. (a) We have $\mathcal{S}_{\{1,2,3\}} = \{\mathbb{1}, g_2\}$, while $\mathcal{S}_{N \subsetneq \{1,2,3\}} = \{\mathbb{1}\}$ for all proper subsets N . Therefore we can detect this structure with three-marginals, but not with two marginals. (b) We have $\mathcal{S}_{\{1,2,3\}} = \{\mathbb{1}, g_1g_2g_3\}$, while $\mathcal{S}_{N \subsetneq \{1,2,3\}} = \{\mathbb{1}\}$ for all proper subsets N . Also here we can detect this structure with three-marginals, but not with two marginals. (c) We have $\mathcal{S}_{\{1,2,3,4\}} = \{\mathbb{1}, g_1, g_4, g_1g_4\}$, $\mathcal{S}_{\{1,4\}} = \{\mathbb{1}, g_1g_4\}$ and $\mathcal{S}_{N \subsetneq \{1,2,3,4\}} = \{\mathbb{1}\}$ for all other proper subsets N . Therefore we can detect some details of the structure with four-marginals, but not with lower number marginals.

LU equivalent graphs G and G' and a set M such that G_M and G'_M are their marginal graphs.

Note that a marginal orbit is less restrictive than a graph orbit. Two not LU equivalent graphs might have the same metagraph.

Corollary 10. *Consider two graphs $G = (V, E)$ and $G' = (V, E')$ defined on the same node set V . If the corresponding graph states $|G\rangle$ and $|G'\rangle$ are LU-equivalent, all pairs of metagraphs belong to the same marginal orbit.*

Marginal orbits of two node sets as well as clustering of two node sets with certain properties were discussed in Ref. [21] (in this reference, it was called the foliage partition). It was shown that metagraphs of sets M of two nodes and $d_M = 1$ belong to the same marginal orbit. It was further shown that metagraphs of general sets M and $d_N = 1$ for all $N \subseteq M$, $|N| = 2$ belong to the same marginal orbit.

While the meta orbit of two node metagraph states G_M can be decided by computing d_M , this is not the case in general. For example for $|M| = 3$, d_M can be 0, 1, or 2, but there are more than three orbits. We can have $d_M = 1$ in two cases: either because we found a two-marginal and added one node, that is $d_N = 1$ for one $N \subsetneq M$ or because we found a new structure, that is $d_N = 0$ for all $N \subsetneq M$. The two cases clearly belong to different marginal orbits. Also, we can have $d_M = 2$ in two cases: either because we found a two-marginal and a new structure in three nodes, that is $d_N = 1$ for one $N \subsetneq M$ or because all subsets of two nodes have an

interesting structure, that is $d_N = 1$ for all $N \subsetneq M$. Also here the two cases clearly belong to different marginal orbits.

We can determine whether $d_M > 0$ indicates a new structure on the whole set M or whether all structures were already detected in subsets of M by comparing stabilisers. We find something new, if and only if the following relation holds:

$$|\mathcal{S}_M| > |\langle \bigcup_{N \subsetneq M} \mathcal{S}_N \rangle|. \quad (34)$$

where $\langle \mathcal{S} \rangle$ denotes the group generated by elements in \mathcal{S} . In the case $|M| = 3$ an equivalent condition is given by

$$d_M > \sum_{N \subset M, |N|=2} d_N, \quad (35)$$

See Fig. 7 for examples of structures which fulfil this condition.

An observation about Eq. (34) is stated in the following lemma. It is closely related to Lemma 1 from [38] and mostly follows from it. For completeness we still give a self-contained proof.

Lemma 11. *For any set M , the relation between the dimensions of a stabiliser set of a marginal state ρ_M and its sub marginals obey the following relation:*

$$|\mathcal{S}_M| = 2^\ell |\langle \bigcup_{N \subsetneq M} \mathcal{S}_N \rangle|, \quad (36)$$

where $\ell \in \{0, 1, 2\}$. Furthermore, if Eq. (36) is satisfied for $\ell = 2$, then the size of M is an even number and $\langle \bigcup_{N \subsetneq M} \mathcal{S}_N \rangle = \{I\}$ and it holds that $|\mathcal{S}_M| = 4$.

App. A contains a proof of the statement. Notice that this relation was recently observed in Ref. [37] for the special case when $|\langle \bigcup_{N \subsetneq M} \mathcal{S}_N \rangle| = 1$.

A straight-forward partition into orbits can be done by computing the stabiliser dimension of the set M and all subsets. A finer partition might be found numerically. Interestingly, for three-node metagraphs the finest numerical partition coincides with the partition found by stabiliser dimensions. We might see a finer partition for larger sets.

IV. DISTINGUISHING LU ORBITS BEYOND THE TOOL OF MARGINAL DIMENSIONS

Our methods can distinguish LU orbits and classes of graphs with up to 8 nodes. The first example where all signatures are identical but the graphs are not LU equivalent are two classes of graphs with 9 nodes. Representatives of these are shown in Fig. 8. The Bouchet algorithm shows that this two graphs are not LC equivalent [15]. But also other methods can be used to prove that they are not LU equivalent.

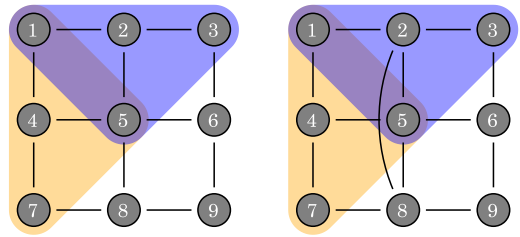


Figure 8. Two nine-qubit graph states L (left) and R (right) that are not LU equivalent. The marginals $\rho_{\{1,2,3,5\}}$ and $\rho_{\{1,4,5,7\}}$ are highlighted in blue and orange, respectively.

Lemma 12. *The graphs L and R are not LU equivalent.*

Proof. Let us compare the stabiliser of marginal $\rho_{\{1,2,3,5\}}$ for both L and R . We find them to be stabilised by

$$S_{\{1,2,3,5\}}^L = \{\mathbb{1}, g_2^L\} = \{\mathbb{1}, Z_1 X_2 Z_3 Z_5\}, \quad (37)$$

$$S_{\{1,2,3,5\}}^R = \{\mathbb{1}, g_1^R g_2^R g_3^R g_5^R\} = \{\mathbb{1}, -Y_1 Y_2 Y_3 Y_5\}, \quad (38)$$

for L and R , respectively; the last equality holds since $XZ = -iY$.

Assume now that there exists a local unitary operation $U = U_1 U_2 U_3 \cdots U_n$ such that $U|L\rangle = |R\rangle$. Notice that

$$U_1 U_2 U_3 U_5 \rho_{\{1,2,3,5\}}^L U_1^\dagger U_2^\dagger U_3^\dagger U_5^\dagger = \rho_{\{1,2,3,5\}}^R,$$

and by Eq. (17) and comparing Eq. (37) and Eq. (38), we then know that $U_1 Z U_1^\dagger = Y$ up to a phase.

On the other hand, for the stabiliser of the marginal $\rho_{\{1,4,5,7\}}$ we find:

$$S_{\{1,4,5,7\}}^L = \{\mathbb{1}, g_4^L\} = \{\mathbb{1}, Z_1 X_4 Z_5 Z_7\}$$

$$S_{\{1,4,5,7\}}^R = \{\mathbb{1}, g_4^R\} = \{\mathbb{1}, Z_1 X_4 Z_5 Z_7\}.$$

Hence, $U_1 Z U_1^\dagger = Z$ up to a phase. This is a contradiction to $U_1 Z U_1^\dagger = Y$ up to a phase. \square

We have found other examples of graphs that have the same signatures but are not LC-equivalent. These are potential candidates for counter-examples to the LC-LU conjecture with a few qubits.

V. TOOLS FOR CHARACTERIZING LC ORBITS

A. Condensed Graphs

With the tools introduced in the previous section, we can detect many structures in graphs. However, due to computational power, we are restricted to certain marginal order. In this section we discuss how to condense graphs such that we can detect some of the structures with marginals of lower order. Condensed graphs were introduced in Ref. [21] as foliage graphs together

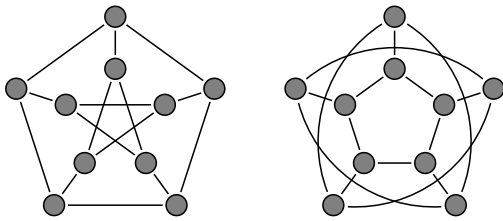


Figure 9. The graph on the left, known as the *Peterson graph*, and the graph on the right have the same T_k for all k . The graphs are related by permutation of the ‘inner’ and ‘outer’ nodes, so they belong to the same class. However, they do not belong to the same LC -orbit.

with a specific condensation rule. Ref. [39] showed that the condensation rule can get relaxed for labeled graphs. After discussing the previous results, we present a generalisation of condensing graphs for labeled and unlabeled graphs. It should be stressed that the tools derived in this section can only prove inequivalence under LC operations, and not under more general LU operations.

By a condensed graph, we mean a graph where we combine a set of vertices of the initial graph into one vertex. The adjacency between the new vertex and the rest of the graph is derived by the adjacency of the set of vertices which got condensed into one vertex and the rest of the graph. We define a condensed graph as follows:

Definition 13. Consider a graph $G = (V, E)$ and a set $C \subseteq V$. The condensed graph $G_C = (V_C, E_C)$ is a graph defined on the node set $V_C = \{c\} \cup (V \setminus C)$, and edge set E_C defined in the following way: $(i, j) \in E_C$ if either $i, j \in V \setminus C$ and $(i, j) \in E$, or $j = c$ and there exists $s \in C$ such that $(i, s) \in E$.

The definition of a graph condensed with respect to multiple sets $\mathcal{C} = \{C\}$ can be formulated analogously.

Some choices of condensation sets C preserve LC equivalence of graphs:

Lemma 14. Given two graphs G and G' and a two node condensation set C such that $d_C = 1$. If G and G' are LC equivalent, it follows that G_c and G'_c are LC equivalent.

Recall that d_C is the marginal dimension of the marginal set C as defined in Eq. (15). This statement was proven for the special case $\mathcal{C} = \{C | d_C = 1\}$ in Ref. [21] and for general two node sets in Ref. [39]. Note that we can use the negated statement to exclude LC equivalence: If the condensed graphs G_c and G'_c are not LC equivalent, also the initial graphs G and G' are not LC equivalent.

While on labeled graphs, the condensation can be done on specific sets, for unlabeled graphs it is challenging to find the same sets on two nodes. Therefore one has to find extra conditions like condensing all sets with a certain property. Practical properties can be “all sets C of size two and $d_C = 1$ ”, as in [21] or “all sets C of size two and

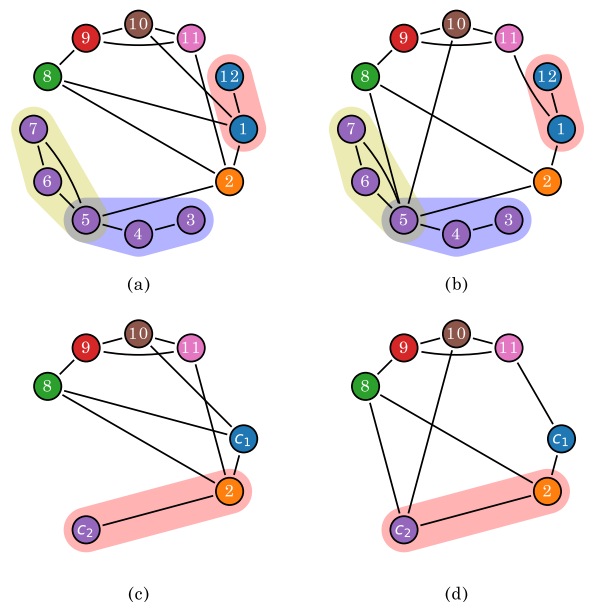


Figure 10. (a) Two 12 node graphs which have all marginal dimensions of two and three node sets equal, that is $L_i^{2,G} = L_i^{2,G'}$ and $L_i^{3,G} = L_i^{3,G'}$ for all $i < 2$ and 3 , respectively. (b) After condensation of sets $\{3, 4, 5, 6, 7\}$ and $\{1, 12\}$, we see that the condensed seven node graphs differ by their marginal dimension $d_{2,3}$. Therefore the two initial graphs are not LC equivalent.

$d_C = 1$ which belong to a cluster of size k ”. An example is shown in Fig. 10.

We show that the condensation sets can be chosen more generally.

Lemma 15. Given two graphs G and G' and a condensation set C such that $d_C = |C| - 1$. If G and G' are LC equivalent, it follows that G_c and G'_c are LC equivalent.

Note that Lem. 14 is a special case of Lem. 15, where $|C| = 2$. In the following we present a proof idea. For the complete proof, see App. B.

Proof idea: We first show that every set C with $d_C = |C| - 1$ has exactly one neighbourhood. That is, there is a neighbourhood \mathcal{N}_C of nodes connected to nodes in C such that C can be composed into two disjoint sets of isolated nodes C_I and nodes which are connected to the neighbourhood C_N such that for all $i \in C_N$ and all $n \in \mathcal{N}_C$ we have that $(i, n) \in E$. We then show that for two graphs which are LC equivalent also the condensed graphs are LC equivalent.

There might be further conditions for condensation graphs, which we present in the following conjecture.

Conjecture 16. Given two graphs G and G' and a condensation set C such that each node in C is connected to at most one node in the neighbourhood in $V \setminus C$. If G and G' are LC equivalent, it follows that G_c and G'_c are LC equivalent.

It would be interesting to find more condensation rules. In App. B we show a list of some trials together with counter examples which show that they do not work.

VI. COMPUTATIONAL COMPLEXITY

In this section we compare the presented methods to existing algorithms and discuss the computational complexity of them. Note that we compute the complexity of the algorithms we used, which is in general an upper bound to the complexity of the best algorithm.

It is possible to decide LU-equivalence by solving a finite set of polynomial equations [8, 40]. However, there is no efficient algorithm known. The Bouchet algorithm which can be used to determine LC equivalence of two graphs has a computational complexity of $\mathcal{O}(n^4)$. Deciding pairwise LC equivalence using Bouchets algorithm scales quadratic in the number of graphs. The presented methods to decide LU equivalence scale linear in the number of graphs. The complexity of our methods up to $k \geq 2$ is upper bounded by $\mathcal{O}(k^{\frac{3}{2}-k}n^{k+1})$. However, for graphs of 9 or more nodes, our methods are only approximations.

In Sec. III, we present the marginal dimension d_M of a subset of nodes M . Although calculating any marginal state of an arbitrary quantum state takes exponentially many steps, the complexity to compute d_M for a given set $|M| = k$ on a graph of n nodes is $\mathcal{O}((n-k)k^2)$. There are $\binom{n}{k}$ subsets $M \subseteq V$ of size k . Using the Stirling approximation, we find that the complexity to compute d_M for all subsets $|M| = k$ on a graph of n nodes is $\mathcal{O}(k^{\frac{3}{2}-k}n^{k+1})$.

In Sec. III A, we introduce the measures $L_i^{k,G}$, and l_k^G and T_k^G . The computational complexity is the same as computing d_M for all subsets $|M| = k$. For the measure t_k , additionally the eigenvalues of a $n \times n$ Hermitian matrix need to be computed, which in practise is $\mathcal{O}(n^3)$. Therefore, to calculate t_k given T_k^G is $\mathcal{O}(n^3)$, while calculating t_k without T_k^G is $\mathcal{O}(n^3)$ for $k = 1$ and $\mathcal{O}(k^{\frac{3}{2}-k}n^{k+1})$ for $k \geq 2$.

In Sec. V, we discuss graph condensation. For the condensation rule given in Lem. 15, we compute the marginal dimensions d_M of all sets M of a certain size $k \geq 2$. Then, we condense the graph, which can be done with a loop over the adjacency matrix in $\mathcal{O}(n^2)$ steps. Therefore also for condensation, the complexity is $\mathcal{O}(k^{\frac{3}{2}-k}n^{k+1})$. Note that condensed graphs have fewer nodes, what makes it computationally easier to compare them. Condensed graphs can get compared with each other or get further condensed.

Note that, however, condensed graphs have fewer nodes, making it computationally easier to compare them. Condensed graphs can get compared with each using the other methods presented in this paper other,

or get further condensed.

VII. SUMMARY AND OUTLOOK

This paper aims at advancing the understanding of the relationship between the marginal state properties and the LU-equivalence of graph states. For that, we introduced an invariant under local unitaries related to the entanglement entropy. We showed how the invariant can be computed in several ways: from the adjacency matrix, from the rank of marginal states, from stabiliser properties, and from geometric graph properties. We then demonstrated how it can be used to distinguish LU-orbits of graph states.

Based on our results, it is both possible to distinguish graph state orbits by computer-implemented algorithms and (often) intuitively by visual inspection of their graphs. We further showed how the problem of deciding LC-equivalence can be mapped to condensed graphs with fewer nodes than the original graphs.

Further research could focus on gaining a better understanding of marginal orbits, particularly in terms of their advantages over computing marginal dimensions of sets with more than three nodes. Additionally, it would be interesting to discover more general condensation rules.

In this paper, we restricted ourselves to local operations being unitary. In general, local operations may include both unitary operations and measurements. Although the problem is addressed in several works [41–45], the structural relationship between which orbits of states can be transformed into which other orbits of states is not yet well understood. It would be interesting to investigate whether our methods can be extended to this more general case.

ACKNOWLEDGMENTS

We thank Jan L. Bönsel, Kiara Hansenne, Lucas E. A. Porto, and Fabian Zickgraf for discussions. This work was supported by the Deutsche Forschungsgemeinschaft (DFG project numbers 447948357, 440958198 and the Emmy Noether grant 418294583), the Sino-German Center for Research Promotion (Project M-0294), the ERC (Consolidator Grant 683107/TempoQ), the German Ministry of Education and Research (Project QuKuK, BMBF Grant No. 16KIS1618K), the Stiftung der Deutschen Wirtschaft, the European Union via the Quantum Internet Alliance project and the BMWK-funded project Qompiler. AB was supported by an NWO Vidi grant (Project No VI.Vidi.192.109). This work is co-funded by the European Union (ERC, ASC-Q, 101040624). Views and opinions expressed are however those of the authors only and do not necessarily reflect those of the European Union or the European Research Council. Neither the European Union nor the granting authority can be held responsible for them.

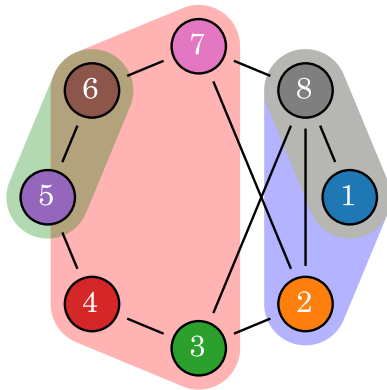


Figure 11. A graph with subsets M such that ℓ in Eq. (A1) takes values 0, 1, and 2. We can find many sets M_0 for which $\ell = 0$, for example $M_0 = \{5, 6\}$ for which both sides of Eq. (A1) are equal to 1. The set $M_1^{\text{even}} = \{1, 8\}$ has a stabiliser of 2 elements. All proper subsets of M_1^{even} have only one stabiliser element which is the identity and therefore we get $\ell = 1$. For $M_1^{\text{odd}} = \{1, 2, 8\}$ we get $\ell = 1$ as well since the stabilisers $\mathcal{S}_{\{1,2,8\}} = \{\mathbb{1}, X_1 Z_8, -Z_1 Y_2 Y_8, -Y_1 Y_2 X_8\}$, $\mathcal{S}_{\{1,8\}} = \{\mathbb{1}, X_1 Z_8\}$ and $\mathcal{S}_N = \{\mathbb{1}\}$ for all other proper subsets $N \subsetneq M_1^{\text{odd}}$. An example where $\ell = 2$ is shown on the marginal set $M_2 = \{3, 4, 6, 7\}$. We have $\mathcal{S}_{\{3,4,6,7\}} = \{\mathbb{1}, X_3 Z_4 Z_6 X_7, Z_3 X_4 X_6 Z_7, Y_3 Y_4 Y_6 Y_7\}$ and $\mathcal{S}_N = \{\mathbb{1}\}$ for all subsets $N \subsetneq M_2$.

Appendix A: Proof of Lemma 11

In this section we prove Lem. 11, which establishes the following relation between the stabiliser set of a marginal state ρ_M and its sub marginals:

$$|\mathcal{S}_M| = 2^\ell |\langle \bigcup_{N \subsetneq M} \mathcal{S}_N \rangle|, \quad (\text{A1})$$

where $\ell \in \{0, 1, 2\}$. Furthermore, if Eq. (A1) is satisfied for $\ell = 2$, then the size of M is an even number and we have $|\mathcal{S}_M| = 4$.

Proof of Lem. 11. Notice that both sets $\langle \bigcup_{N \subsetneq M} \mathcal{S}_N \rangle$ and \mathcal{S}_M are subgroups of the Pauli group and hence their order is a power of two. Moreover, $\langle \bigcup_{N \subsetneq M} \mathcal{S}_N \rangle$ is a subgroup of \mathcal{S}_M , hence $|\mathcal{S}_M| = 2^\ell |\langle \bigcup_{N \subsetneq M} \mathcal{S}_N \rangle|$ for some natural number $\ell \in \mathbb{N}_0$.

We show in Fig. 11 by example that ℓ can take all values in $\{0, 1, 2\}$. We first show that $\ell \geq 3$ is not possible in general. We continue by proving conditions on M and \mathcal{S}_M for $\ell = 2$. We proof all statements by contradiction.

We now show that $\ell \geq 3$ is impossible in general. First, assume $\ell \geq 1$. Therefore, there is a Pauli string $\sigma_1 \in \mathcal{S}_M$ for which $\sigma_1 \notin \langle \bigcup_{N \subsetneq M} \mathcal{S}_N \rangle$ and thus σ_1 has full support on the marginal M . The set $\sigma_1 \langle \bigcup_{N \subsetneq M} \mathcal{S}_N \rangle$ forms a coset of the subgroup $\langle \bigcup_{N \subsetneq M} \mathcal{S}_N \rangle \in \mathcal{S}_M$. Now assume that $\ell \geq 2$. This implies the existence of some Pauli string $\sigma_2 \in \mathcal{S}_M$ that is neither contained in $\langle \bigcup_{N \subsetneq M} \mathcal{S}_N \rangle$ nor in $\sigma_1 \langle \bigcup_{N \subsetneq M} \mathcal{S}_N \rangle$ (i.e. the coset of σ_1). In particular, this implies the following: First, let $\sigma_1 = \bigotimes_{i \in V} P_i$ and $\sigma_2 = \bigotimes_{i \in V} Q_i$ for $P_i, Q_i \in \{X, Y, Z\}$. The above implies that $Q_i \neq P_i$ for every $i \in V$, for otherwise we would have $\sigma_1 \sigma_2 \in \mathcal{S}_N$ for some $N \subsetneq M$, which is a contradiction.

Finally, assume $\ell \geq 3$. By the same reasoning as before, this implies the existence of a Pauli string $\sigma_3 \in \mathcal{S}_M$ that is not in the sets $\langle \bigcup_{N \subsetneq M} \mathcal{S}_N \rangle \in \mathcal{S}_M$, $\sigma_1 \langle \bigcup_{N \subsetneq M} \mathcal{S}_N \rangle \in \mathcal{S}_M$, or $\sigma_2 \langle \bigcup_{N \subsetneq M} \mathcal{S}_N \rangle \in \mathcal{S}_M$. Similarly as before, σ_3 has full support on M and has to be different from σ_1 and σ_2 on every position. Because of product relations of Pauli matrices, it follows that $\sigma_3 = \pm \sigma_1 \sigma_2$, which is in contradiction with the assumption that σ_1, σ_2 , and σ_3 are independent. Therefore $\ell = 3$ is not possible.

We continue by showing that if $|M|$ is odd, we can not have $\ell = 2$. We see that because of commutation relations of the Paulis, if $|M|$ is odd, we have $\sigma_1 \sigma_2 = -\sigma_2 \sigma_1$ which contradicts the Abelian structure of \mathcal{S}_M . Therefore for odd sets M , we can not find different stabilisers σ_1 and σ_2 with full support on M and therefore $\ell = 2$ is not possible.

We finally show that if $\ell = 2$, we have $\langle \bigcup_{N \subsetneq M} \mathcal{S}_N \rangle = \{\mathbb{1}\}$. Suppose that there exist an element $\tau \in \langle \bigcup_{N \subsetneq M} \mathcal{S}_N \rangle$ where $\tau \neq \mathbb{1}$. As stated before, when $\ell = 2$ there exist elements σ_1, σ_2 and $\sigma_3 = \sigma_1 \sigma_2$ that have all different Pauli operators on all nodes. Since $\tau \neq \mathbb{1}$, there is at least one node on which τ has non-trivial support. But then, at least $\tau \sigma_1, \tau \sigma_2$, or $\tau \sigma_3$ does not have full support; w.l.o.g. assume this is so for $\tau \sigma_1$. However, then τ and $\tau \sigma_1$ are both in $\langle \bigcup_{N \subsetneq M} \mathcal{S}_N \rangle$, which is in direct contradiction with the fact that $\sigma_1 = \tau^2 \sigma_1 \notin \langle \bigcup_{N \subsetneq M} \mathcal{S}_N \rangle$. Therefore, no such τ can exist and it must be that $\langle \bigcup_{N \subsetneq M} \mathcal{S}_N \rangle = \{\mathbb{1}\}$. \square

Appendix B: Condensation Rules

1. Proof of Lemma 15

In this section, we prove Lem. 15 which states that given two graphs G and G' and a condensation set C such that $d_C = |C| - 1$ then, if G and G' are LC equivalent, it follows that G_c and G'_c are LC equivalent. We first introduce notation.

Consider a graph $G = (V, E)$ and a set $C \subsetneq V$ such that $d_C = |C| - 1$. We earlier defined the neighbourhood of a set \mathcal{N}_C as the set of vertices adjacent to vertices in C . In Def. 2, we defined metagraphs. For a graph G and a set C , we defined the metagraph G_C which has two type of nodes. Type-1 nodes are those from set C , while type-2 nodes represent some nodes outside of C and tell whether they are connected to a certain subset B of C . Here, we are interested in the set of nodes in $V \setminus C$ which get represented by type-2 nodes. We denote this set $\hat{\mathcal{N}}_B$ and define it such that all nodes in $B \in \mathcal{P}(C) \setminus \emptyset$ are adjacent with all vertices in $\hat{\mathcal{N}}_B$ and B is the largest subset of C for which this is true:

$$\hat{\mathcal{N}}_B := \left\{ v \in V \setminus C \mid \begin{array}{l} \forall b \in B : (v, b) \in E \text{ and} \\ \forall c \in C \setminus B : (v, c) \notin E \end{array} \right\}. \quad (\text{B1})$$

We call such subset of the complete neighbourhood a neighbourset of B . By definition, we have

$$\mathcal{N}_C = \bigcup_{B \in \mathcal{P}_{k \geq 1}(C)} \hat{\mathcal{N}}_B. \quad (\text{B2})$$

Note that for most $B \subseteq C$, $\hat{\mathcal{N}}_B = \emptyset$. We count how many sets $\hat{\mathcal{N}}_B$ are non-empty and call this number the amount of non-empty neighbourhoods of C .

The proof is divided into two parts. (i) We first show that every set C with $d_C = |C| - 1$ has exactly one non-empty neighbourhood. That is, there is a $B \subseteq C$, $B \neq \emptyset$ such that $\mathcal{N}_C = \hat{\mathcal{N}}_B$ if and only if $d_C = |C| - 1$. (ii) We then show that for two graphs which are LC equivalent also the condensed graphs are LC equivalent.

Proof. (i) $\exists B \subseteq C$, $B \neq \emptyset$: $\mathcal{N}_C = \hat{\mathcal{N}}_B \Leftrightarrow d_C = |C| - 1$.

\Rightarrow Consider a set $C \subseteq V$ with a neighbourhood \mathcal{N}_C and a set $B \subseteq C$ with $B \neq \emptyset$ such that $\hat{\mathcal{N}}_B = \mathcal{N}_C$. We count the number of elements in the stabiliser set \mathcal{S}_C and compute d_C from this number. The stabiliser set is a subset of the set generated by all generators g_i for $i \in C$:

$$\mathcal{S}_C \subseteq \langle \{g_i \mid i \in C\} \rangle, \quad (\text{B3})$$

and therefore the number of elements in \mathcal{S}_C is upper bounded by $2^{|C|}$.

Consider the case where $B = \{b\}$, that is, B contains only one element. We have that $\text{tr}_{V \setminus B}(g_c) = g_c$ for all $c \in C \setminus B$. Therefore $\langle g_c \mid c \in C \setminus B \rangle \subseteq \mathcal{S}_C$ and therefore \mathcal{S}_C has at least $2^{|C|-1}$ elements. Further we have $\text{tr}_{V \setminus B}(g_b) = 0$ and therefore $g_b \notin \mathcal{S}_C$. Also all products containing g_b are not in \mathcal{S}_C , which are $2^{|C|-1}$ terms. Therefore \mathcal{S}_C has at most $2^{|C|} - 2^{|C|-1} = 2^{|C|-1}$ elements. It follows that \mathcal{S}_C has exactly $2^{|C|-1}$ elements, which corresponds to $d_C = |C| - 1$.

For $|B| > 1$ a similar argumentation can be made. We have that $\text{tr}_{V \setminus B}(g_c) = g_c$ for all $c \in C \setminus B$, which are $|C| - |B|$ elements. Also $g_b g_{b'} \in \mathcal{S}_C$ for all $b, b' \in B$, $b \neq b'$, which are $|B| - 1$ (algebraically) independent elements. Therefore \mathcal{S}_C has at least $2^{(|C|-|B|)+(|B|-1)} = 2^{|C|-1}$ elements. Further, all products of generators which contain an odd number of generators g_b , $b \in B$ are not in \mathcal{S}_C . This are $2^{|C|-1}$ elements. Therefore \mathcal{S}_C contains exactly $2^{|C|-1}$ elements, which corresponds to $d_C = |C| - 1$.

\Leftarrow Proof by contradiction. Assume that C has more than one non-empty neighbourhood. That is there are two sets $B_1, B_2 \in C$, both not empty and $B_1 \neq B_2$ which have a non-empty neighbourhood: $\hat{\mathcal{N}}_{B_1} \cup \hat{\mathcal{N}}_{B_2} \subseteq \mathcal{N}_C$. This is the case if C has at least two non-empty neighbourhoods. There are three relevant relations between B_1 and B_2 . We show that in all cases $d_C < |C| - 1$.

- a) $B_1 \cap B_2 = \emptyset$: All products of stabiliser elements which contain odd numbers of generators g_b , $b \in B_1$ are not in \mathcal{S}_C , which are $2^{|C|-1}$ elements. There is at least one more product of generators which contains an odd number of generators g_b , $b \in B_2$. Therefore $|\mathcal{S}_C| \leq 2^{|C|-1} - 1$ and therefore $d_C < |C| - 1$.
- b) $B_1 \subsetneq B_2$: ($B_2 \subsetneq B_1$ equivalent.) Same argumentation as in (a) for the disjoint sets B_1 and $B_2 \setminus B_1$.
- c) $B_1 \cap B_2 \neq \emptyset, B_1 \not\subseteq B_2, B_2 \not\subseteq B_1$: Same argumentation as in (a) for the disjoint sets $B_1 \setminus B_2$ and $B_2 \setminus B_1$.

Therefore, if C has more than one non-empty neighbourhood, we have $d_C < |C| - 1$.

It follows that it is equivalent that C has exactly one non-empty neighbourhood and $d_C = |C| - 1$.

(ii) We show that for two graphs G and G' which are LC equivalent the condensed graphs G_C and G'_C are also equivalent where C is chosen such that $d_C = |C| - 1$. Without loss of generality we assume that there is a $j \in V$ such that $G' = \text{LC}_j(G)$, otherwise the argumentation has to be applied multiple times.

We divide the node set V into four disjoint sets:

$$V = B \dot{\cup} (C \setminus B) \dot{\cup} \mathcal{N}_C \dot{\cup} (V \setminus (C \cup \mathcal{N}_C)). \quad (\text{B4})$$

As shown in (i), for the chosen set C we have $\mathcal{N}_C = \hat{\mathcal{N}}_B$. We show that for local complementation on any node in one of the sets, the statement is true.

- a) $j \in V \setminus (C \cup \mathcal{N}_C)$: Local complementation on a node which is not adjacent to C , does not change the structure of the graph in the set C and therefore has the same effect on a graph before and after condensation. That is $G'_C = \text{LC}_j(G_C)$.
- b) $j \in C \setminus B$: Local complementation can only changes the connectivity structure in C , what we do not see after condensation. That is $G'_C = G_C$.
- c) $j \in B$: Local complementation can change the edge structure of C , of \mathcal{N}_C as well as the set B to another set $B' \neq \emptyset$. Changes in C have no effect. Changes in \mathcal{N}_C are the same as local complementation on node c on G_C . The change of B is such that $\hat{\mathcal{N}}_B = \hat{\mathcal{N}}_{B'}$, that is C still has exactly one non-empty neighbourhood which is the same as before. That is $G'_C = \text{LC}_c(G_C)$.
- d) $j \in \mathcal{N}_C$: Local complementation can change the edge structure in C , which does not matter for condensation. It further can change the neighbourhood of C in the same way as it changes the neighbourhood of c in the condensed graph. It can also change other edges which are not affected by condensation in C . That is $G'_C = \text{LC}_j(G_C)$.

Therefore in all cases G_C and G'_C are LC equivalent after condensation. □

2. Not Working Condensation Rules

Below we give a list of condensation rules which are not sufficient to help deciding LC-equivalence of the initial graphs.

Observation 17. *We give a list of condensation rules which preserve LC-equivalence in some cases but do not hold in full generality.*

1. *It is not correct that a set C can be condensed whenever $|\mathcal{S}_C| > |\langle \bigcup_{B \subseteq C} \mathcal{S}_B \rangle|$ is fulfilled.*
2. *A condensation set C with a neighbourhood which can get composed into neighboursets which are not adjacent by a path outside C can not be condensed in general.*
3. *It is not true that a set C such that the neighbourhood can get composed into non-empty neighboursets $\hat{\mathcal{N}}_D$ for some $D \in \mathcal{D}$ where all $D \in \mathcal{D}$ are pairwise disjoint can be condensed in general. \mathcal{D} is the set of $D \subseteq C$ for which the neighbourset is not empty.*

Counterexamples are shown in Fig. 12.

-
- [1] G. Murta, F. Grasselli, H. Kampermann, and D. Bruß, *Adv. Quantum Technol.* **3**, 2000025 (2020).
[2] R. Raussendorf, D. E. Browne, and H. J. Briegel, *Phys. Rev. A* **68**, 022312 (2003).
[3] B. M. Terhal, *Rev. Mod. Phys.* **87**, 307 (2015).
[4] R. Horodecki, P. Horodecki, M. Horodecki, and K. Horodecki, *Rev. Mod. Phys.* **81**, 865 (2009).
[5] O. Gühne and G. Tóth, *Physics Reports* **474**, 1 (2009).
[6] M. Hein, W. Dür, J. Eisert, *et al.*, *Proceedings of the International School of Physics “Enrico Fermi”* **162**, 115 (2006).
[7] B. Kraus, *Phys. Rev. Lett.* **104**, 020504 (2010).
[8] T. Maciążek, M. Ozmaniec, and A. Sawicki, *J. Math. Phys.* **54**, 092201 (2013).

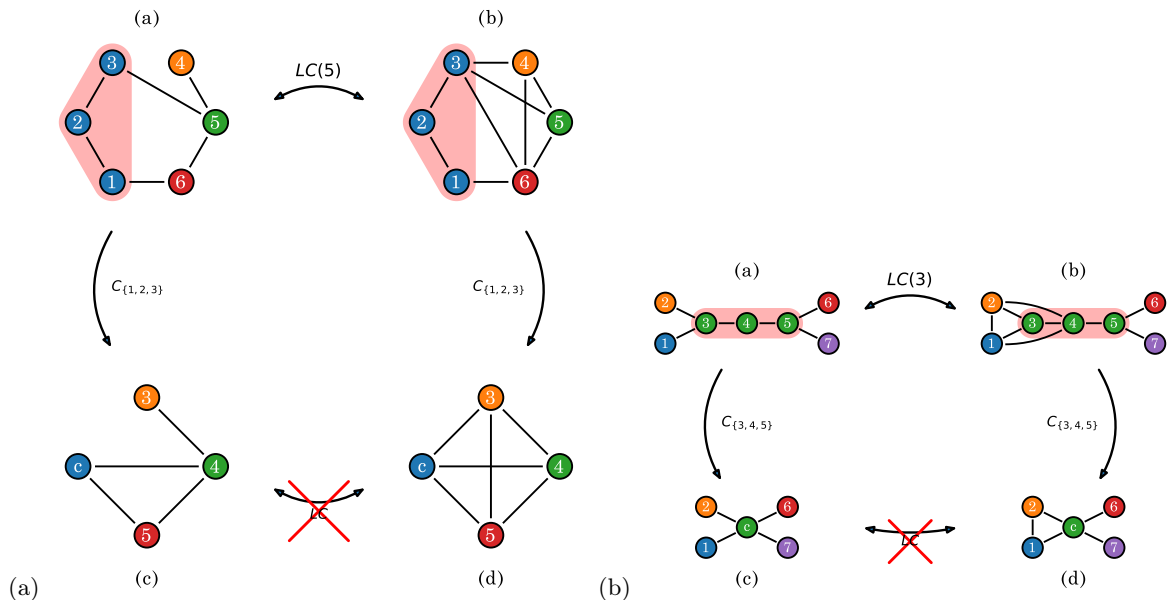


Figure 12. Counterexamples for not working condensation rules, presented in Observation 17. In both cases we chose a condensation set C such that $d_C = 1$ and Eq. (34) is fulfilled. In (b) we have additionally that the neighboursets $\hat{\mathcal{N}}_3 = \{1, 2\}$ $\hat{\mathcal{N}}_5 = \{6, 7\}$ are not adjacent by a path outside C and that $\{3\}$ and $\{5\}$ are disjoint.

- [9] M. Van den Nest, J. Dehaene, and B. De Moor, *Phys. Rev. A* **69**, 022316 (2004).
- [10] D. Gross and M. V. den Nest, The LU-LC conjecture, diagonal local operations and quadratic forms over GF(2) (2007), [arXiv:0707.4000](https://arxiv.org/abs/0707.4000).
- [11] Z. Ji, J. Chen, Z. Wei, and M. Ying, *Quantum Inf. Comput.* **10**, 97 (2010).
- [12] N. Tsimakuridze and O. Gühne, *J. Phys. A Math. Theor.* **50**, 195302 (2017).
- [13] A. Cabello, A. J. López-Tarrida, P. Moreno, and J. R. Portillo, *Phys. Lett. A* **373**, 2219 (2009).
- [14] A. Dahlberg, J. Helsen, and S. Wehner, *J. Math. Phys.* **61**, 022202 (2020).
- [15] A. Bouchet, *Discrete Math.* **114**, 75 (1993).
- [16] M. Van den Nest, J. Dehaene, and B. De Moor, *Phys. Rev. A* **70**, 034302 (2004).
- [17] M. Hein, J. Eisert, and H. J. Briegel, *Phys. Rev. A* **69**, 062311 (2004).
- [18] M. Hajdušek and M. Murao, *New J. Phys.* **15**, 013039 (2013).
- [19] A. Burchardt and Z. Raissi, *Phys. Rev. A* **102**, 022413 (2020).
- [20] Z. Raissi, A. Burchardt, and E. Barnes, *Phys. Rev. A* **106**, 062424 (2022).
- [21] A. Burchardt and F. Hahn, The foliage partition: An easy-to-compute LC-invariant for graph states (2023), [arXiv:2305.07645](https://arxiv.org/abs/2305.07645).
- [22] D. M. Greenberger, M. A. Horne, and A. Zeilinger, Going beyond Bell's theorem, in *Bell's Theorem, Quantum Theory and Conceptions of the Universe*, edited by M. Kafatos (Springer, 1989) pp. 69–72.
- [23] M. Proietti, J. Ho, F. Grasselli, *et al.*, *Sci. Adv.* **7**, eabe0395 (2021).
- [24] M. Epping, H. Kampermann, D. Bruß, *et al.*, *New J. Phys.* **19**, 093012 (2017).
- [25] M. Hillery, V. Bužek, and A. Berthiaume, *Phys. Rev. A* **59**, 1829 (1999).
- [26] F. Hahn, J. de Jong, and A. Pappa, *PRX Quantum* **1**, 020325 (2020).
- [27] L. Rüdckle, J. Budde, J. de Jong, *et al.*, *Phys. Rev. Res.* **5**, 033222 (2023).
- [28] R. Raussendorf and H. J. Briegel, *Phys. Rev. Lett.* **86**, 5188 (2001).
- [29] M. A. Nielsen, *Rep. Math. Phys.* **57**, 147 (2006).
- [30] M. Van den Nest, J. Dehaene, and B. De Moor, *Phys. Rev. A* **69**, 022316 (2004).
- [31] M. Van den Nest, J. Dehaene, and B. De Moor, *Phys. Rev. A* **70**, 034302 (2004).
- [32] O. Gittsovich, P. Hyllus, and O. Gühne, *Phys. Rev. A* **82**, 032306 (2010).
- [33] N. Wyderka and O. Gühne, *J. Phys. A Math. Theor.* **53**, 345302 (2020).
- [34] H.-T. Nguyen and S. il Oum, *Eur. J. Comb.* **90**, 103183 (2020).
- [35] P. Høyer, M. Mhalla, and S. Perdrix, in *Algorithms and Computation*, edited by T. Asano (Springer, 2006) pp. 638–649.
- [36] A. Cabello, L. E. Danielsen, A. J. López-Tarrida, and J. R. Portillo, *Physical Review A* **83**, 042314 (2011), publisher: American Physical Society.
- [37] N. Claudet and S. Perdrix, Covering a graph with minimal local sets (2024), [arXiv:2402.10678](https://arxiv.org/abs/2402.10678).
- [38] M. V. d. Nest, J. Dehaene, and B. De Moor, *Physical Review A* **71**, 062323 (2005), [arXiv:quant-ph/0411115](https://arxiv.org/abs/quant-ph/0411115).
- [39] D. Zhang, Bell pair extraction using graph foliage techniques (2023), [arXiv:2311.16188](https://arxiv.org/abs/2311.16188).
- [40] B. Kraus, *Phys. Rev. A* **82**, 032121 (2010).

- [41] F. Hahn, A. Pappa, and J. Eisert, [npj Quantum Inf.](#) **5**, 76 (2019).
- [42] V. Mannalath and A. Pathak, [Phys. Rev. A](#) **108**, 062614 (2023).
- [43] J. de Jong, F. Hahn, N. Tcholtchev, *et al.*, [Phys. Rev. Res.](#) **6**, 013330 (2024).
- [44] S. Brand, T. Coopmans, and A. Laarman, Quantum graph-state synthesis with SAT (2023), [arXiv:2309.03593](#).
- [45] K. Szymański, L. Vandr e, and O. G uhne, Useful entanglement can be extracted from noisy graph states (2024), [arXiv:2402.00937](#).